Crystal structure of antimony oxalate hydroxide, $Sb(C_2O_4)OH$

James A. Kaduk,[a] Mark A. Toft, and Joseph T. Golab
INEOS Technologies, P.O. Box 3011, MC F-9, Naperville, Illinois 60566

(Received 14 September 2009; accepted 5 November 2009)

The crystal structure of $Sb(C_2O_4)OH$ has been solved by charge flipping in combination with difference Fourier techniques using laboratory X-ray powder data exhibiting significant preferred orientation and refined by the Rietveld method. The compound crystallizes in *Pnma* with $a=5.827\ 13(3)$, $b=11.294\ 48(10)$, $c=6.313\ 77(3)$ Å, $V=415.537(5)$ Å^3, and $Z=4$. The crystal structure contains pentagonal pyramidal Sb^{3+} cations, which are bridged by hydroxyl groups to form zigzag chains along the *a* axis. Each oxalate anion chelates to two Sb in approximately the *ab* plane, linking the chains into a three-dimensional framework. The H of the hydroxyl group is probably disordered in order to form stronger more-linear hydrogen bonds. The highest energy occupied molecular orbitals are the Sb^{3+} lone pairs. The structure is chemically reasonable compared to other antimony oxalates and to $Bi(C_2O_4)OH$. © *2010 International Centre for Diffraction Data.* [DOI: 10.1154/1.3308616]

Key words: Antimony, oxalate, hydroxide, crystal structure, Rietveld refinement, charge flipping

I. INTRODUCTION

Some of the reagents used to synthesize Sb-containing catalysts are variable in composition, hampering reproducible catalyst preparation. As part of a program to generate stoichiometric reagents, antimony oxalate hydroxide was prepared. Its crystal structure was solved by applying the charge flipping method (Oszlányi and Sűtó, 2008) and difference Fourier techniques to laboratory X-ray powder diffraction data and refined by the Rietveld (1969) method. Density functional calculations were used to understand the bonding.

II. EXPERIMENTAL

A. Sample preparation

Sb_2O_3 (25 g) and oxalic acid dihydrate (22 g) were slurried in 300 ml de-ionized water. The mixture was then refluxed for 3 h. After cooling, the resulting slurry was filtered to recover the $Sb(C_2O_4)OH$ product. The white solid was washed several times with de-ionized water and dried at 110 °C for 3 h. A 96% yield was obtained. The compound has been prepared previously by reaction of oxalic acid dihydrate and $SbCl_3$ (Korzun *et al.*, 2005; Karlov *et al.*, 1983; Ambe, 1975).

B. Powder pattern

The white powder was examined as synthesized. The X-ray pattern was measured (Cu $K\alpha$ radiation, 40 kV, 40 mA, 5° to 150° 2θ in 0.007 296 89° steps, 1 s/step) from a rotating specimen on a Bruker D8 Advance diffractometer equipped with a VÅNTEC-1 position-sensitive detector. Several weak Cu $K(\beta)$ peaks were present in the pattern and were ignored in data processing. A search of the Powder Diffraction File (Faber and Fawcett, 2002) using JADE 8.5 (Materials Data, Inc., 2008) indicated that the product was single-phase $Sb(C_2O_4)OH$ (Karlov *et al.*, 1983) (Figure 1).

The pattern could be indexed using DICVOL06 (Louër and Boultif, 2007) on a high-quality [$M(19)=123.3$, $F(19)=141.1$] orthorhombic unit cell having $a=5.827\ 13(3)$, $b=11.294\ 48(10)$, $c=6.313\ 77(3)$ Å, and $V=415.537(5)$ Å^3. Systematic absences were consistent with space groups *Pnma* or $Pn2_1a$. With $Z=4$, the calculated density was 3.625 g cm^{-3}.

C. Structure solution

Attempts to solve the structure using Monte Carlo simulated annealing and direct method techniques were unsuccessful. Both methods yielded the Sb atom position but no other plausible atoms or fragments. Even Monte Carlo simulated annealing trials using Sb-OH and oxalate fragments were unsuccessful. We attribute these failures to the unrecognized preferred orientation, which tended to concentrate the electron density in the mirror plane.

Structure factors from a Le Bail (2008) extraction carried out using GSAS (Larson and Von Dreele, 2004) were used to create a SHELX HKLF 4 file, which was used as input to SUPERFLIP as incorporated into JANA2006 (Petříček *et al.*, 2006). The Sb and hydroxyl oxygen positions were identified easily. These two atoms were fixed in GSAS, and a difference Fourier map yielded the positions of the oxalate C and one of the O. Another O (the strongest peak in the difference map) was located only 1.06 Å from the Sb but in a direction expected for the remaining oxalate O. This atom was moved manually into approximately the correct position and refinement begun.

D. Refinement

The 15° to 150° portion of the pattern was used in the Rietveld refinement, with excluded regions 18.4° to 20.2°, 25.2° to 25.7°, and 40.5° to 40.9° to eliminate the strongest $K\beta$ peaks. The background was described by a three-term shifted Chebyshev polynomial combined with a nine-term

[a]Electronic mail: kaduk@polycrystallography.com

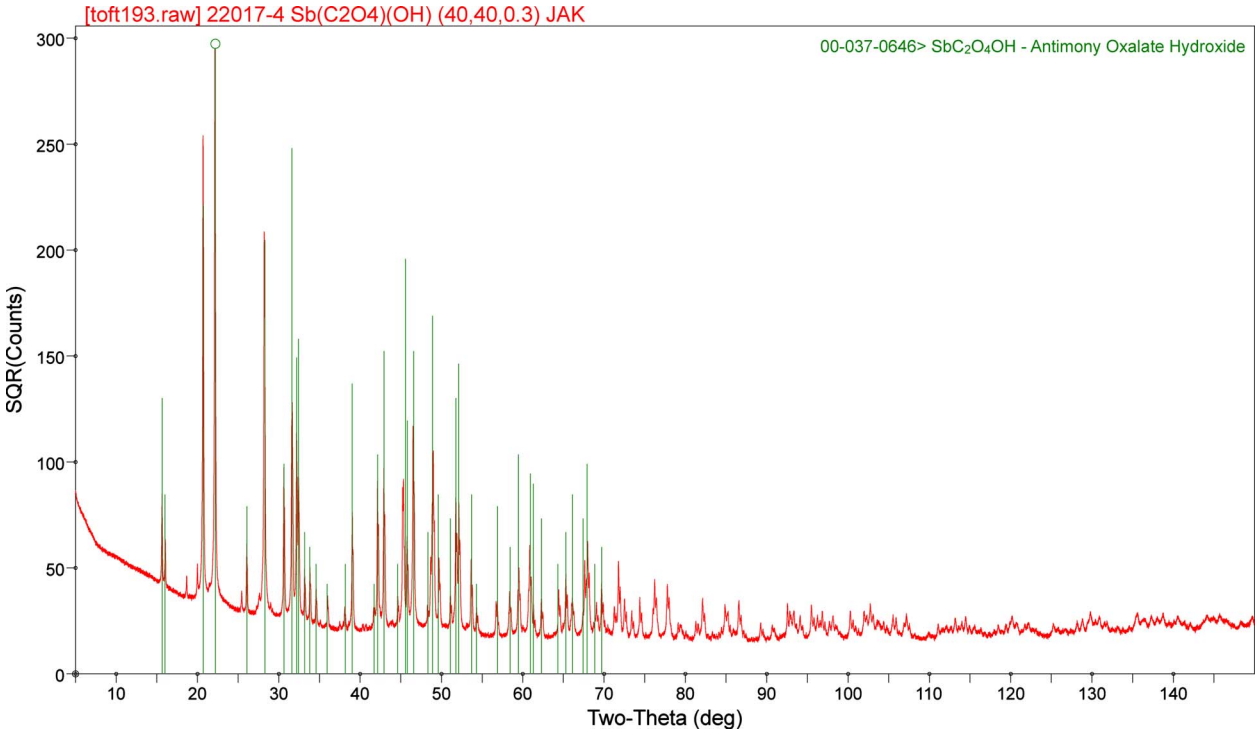

Figure 1. (Color online) Observed X-ray powder pattern of $Sb(C_2O_4)OH$. The vertical scale is $(counts)^{1/2}$ to emphasize the weaker peaks.

diffuse scattering function to describe the small concentration of amorphous material. The peak profiles were described using GSAS profile function No. 4, which includes the Stephens (1999) anisotropic strain broadening model. The $S(040)$ coefficient was fixed at 0, and X and *shft* were also refined. The significant preferred orientation was described by a sixth-order spherical harmonic expansion; the final texture index was 1.441.

The Sb was refined anisotropically, while a common U_{iso} was refined for the O and C atoms. The U_{iso} of the hydrogen atoms was fixed at 1.3 times that of the O/C. Restraints (soft constraints) were applied to the Sb-O bond distances: Sb1-O2=2.00(5) and 2.42(5); Sb1-O3/O4=2.25(5) Å. The bonded [C5-C5=1.55(4), C5-O3/O4=1.25(3) Å] and nonbonded [C5-O3/O4=2.32(5) Å] distances in the oxalate anion were also restrained. An angle restraint O3-C5-O4 =126(5)° was also applied. The restraints contributed 0.9% to the final reduced χ^2.

In space group *Pnma*, the hydroxyl group O2-H6 lies on the mirror plane at $y=1/4$. This results in rather weak and distorted O2-H6···O4 hydrogen bonds to two symmetry-equivalent O4 (Table I). Refinements in subgroups of *Pnma* such as $Pn2_1a$ were unstable (they diverged). A quantum chemical geometry optimization in $Pn2_1a$ led to a structure 93.8 kcal/mol lower in energy, with stronger and more-linear ordered hydrogen bonds (Table I). Refinement of ordered and disordered hydrogen models in *Pnma* yielded the same residuals. The final half-occupancy hydrogen position was therefore fixed off the mirror plane.

The final refinement of 49 variables using 18 139 observations yielded the residuals $R_{wp}=0.0757$, $R_p=0.0604$, $\chi^2=5.651$, $R(F)=0.0837$, and $R(F^2)=0.0964$. The largest peak in the difference Fourier map was $+2.8e$ Å^{-3} (1.03 Å from Sb1) and the largest difference hole was $-2.9e$ Å^{-3} (0.33 Å from Sb1). The largest errors in the final Rietveld plot (Figure 2) are in the shapes of the strong low-angle peaks and the

TABLE I. Disordered and ordered hydrogen bonds in $Sb(C_2O_4)OH$.

Space group	O2-H6 (Å)	H6···O4 (Å)	O2···O4 (Å)	O2-H6···O4 (deg)	Overlap, e
$Pnma\times2$	0.986	2.116	2.958	142.3	0.02
$Pn2_1a$	0.994	1.873	2.865	175.9	0.06

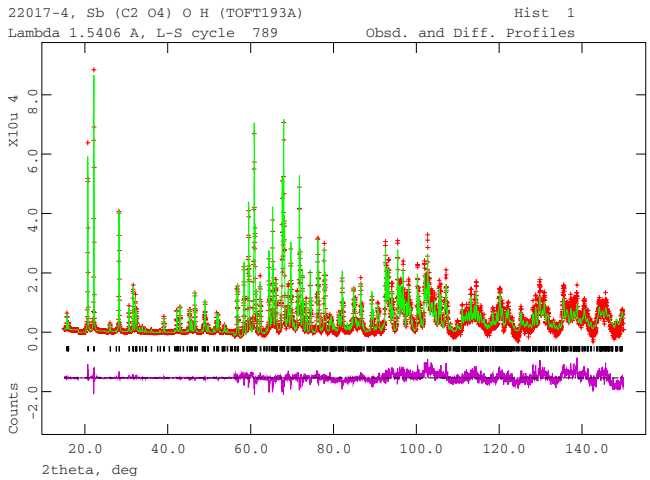

Figure 2. (Color online) The final Rietveld plot for $Sb(C_2O_4)OH$. The red crosses represent the observed data points and the solid green curve; in magenta below is the calculated pattern. The difference pattern in magenta is plotted at the same scale as the other patterns. The row of tick marks indicates the calculated reflection positions. The vertical scale has been magnified by a factor of 20 in the 56° to 89° region and by a factor of 40 from 89° to 150°.

https://doi.org/10.1154/1.3308616 Published online by Cambridge University Press

TABLE II. Refined (top) and optimized (bottom) structural parameters for $Sb(C_2O_4)OH$. Space group *Pnma*, a=5.827 13(3), b=11.294 48(10), and c=6.313 77(3) Å.

Atom	x	y	z	Frac	U_{iso} (Å^2)
Sb1	0.180 70(7)	$\frac{1}{4}$	0.507 64(10)	1	0.0316[a]
	0.195 362	$\frac{1}{4}$	0.508 689		
O2	0.5416(7)	$\frac{1}{4}$	0.7087(5)	1	0.0355(6)
	0.538 432	$\frac{1}{4}$	0.699 660		
O3	0.2500(5)	0.4443(4)	0.6046(4)	1	0.0355
	0.263 354	0.451 844	0.604 577		
O4	0.1180(4)	0.6329(3)	0.5782(4)	1	0.0355
	0.118 971	0.636 388	0.579 989		
C5	0.1102(5)	0.5328(4)	0.5510(6)	1	0.0355
	0.109 424	0.524 306	0.551 501		
H6	0.652 328	0.287 710	0.593 715	$\frac{1}{2}$	0.0455

[a]$U11$=0.0352(3), $U22$=0.0232(7), $U33$=0.0323(3), $U12$=0, $U13$=0.0016(4), and $U23$=0.

high-angle background. The refined and optimized structural parameters are reported in Table II, and bond distances and angles are contained in Tables III and IV.

E. Quantum mechanics

Quantum chemical geometry optimizations were carried out using density functional plane wave pseudopotential techniques as implemented in CASTEP (Clark *et al.*, 2005). The Perdew-Burke-Enzerhof functional with a 300 eV plane wave basis set cutoff was used with lattice parameters fixed at the experimental values. The Brillouin zone was sampled using four k points.

III. RESULTS AND DISCUSSION

The crystal structure contains pentagonal pyramidal Sb^{3+} cations, which are bridged by hydroxyl groups to form zigzag chains along the a axis (Figure 3). Each oxalate anion chelates to two Sb in approximately the ab plane, linking the chains into a three-dimensional framework (Figure 4).

The apical Sb-OH bond is relatively short [1.933(3) Å], while the other Sb-OH bond in the basal plane is relatively long [2.456(2) Å]. The Sb-oxalate bonds are slightly longer than expected from bond valence calculations (2.23 Å) (Brese and O'Keefe, 1991), but the Sb bond valence sum of 3.03 is very close to the expected value. The Sb coordination is "one sided;" the Sb lies 0.80 Å out of the pentagonal plane, as might be expected for a coordination sphere which includes a lone pair.

In the bond valence method (Brown, 2002), the bond valence is most often calculated as $s=\exp[(r_0-r_{obs})/b]$, though other expressions have been used. In the most commonly used tabulation of bond valence parameters (Brese and O'Keefe, 1991), r_0 is tabulated for many cation-anion pairs and b is a universal constant equal to 0.37. For some cations which contain lone pairs, these default values might not be appropriate (Sidey, 2009), and alternate values have been derived. For this compound, both sets of parameters yield reasonable values for the Sb atomic valence (Table III).

The oxalate bond distances and angles fall within the normal ranges (Bruno *et al.*, 2004). The oxalate anion is planar to within 0.01 Å; the mean plane is approximately $(\bar{5},\bar{2},11)$. The disordered hydroxyl group O2-H6 forms a normal-strength hydrogen bond to the oxalate oxygen O4, consistent with the shorter C5-O4 distance and higher calculated charge (O3=−0.56 and O4=−0.62).

The Mulliken overlap populations (Table III) show that the short Sb-OH and the Sb-oxalate bonds have significant covalent character, while the long Sb-OH bond is nearly ionic. Although a ball-and-stick rendering of the structure

TABLE III. Bond distances in $Sb(C_2O_4)OH$.

Bond	GSAS (Å)	CASTEP (Å)	Mulliken overlap population, e
Sb1-O2	1.966(3)	2.056	0.29
	2.456(2)	2.335	0.02
Sb1-O3×2	2.314(4)	2.392	0.14
Sb1-O4×2	2.252(3)	2.305	0.12
Bond valence sum			
Brese and O'Keefe, 1991			
r_0=1.923, b=0.37	3.03	2.64	
Sidey, 2009			
r_0=1.924, b=0.47	3.10	2.80	
C5-O3	1.258(4)	1.260	0.94
C5-O4	1.245(5)	1.280	0.86
C5-C5	1.534(5)	1.533	0.75

TABLE IV. Bond angles in $Sb(C_2O_4)OH$.

Angle	GSAS, °	CASTEP, °
O2-Sb1-O2	83.23(6)	85.31
O2-Sb1-O3×2	73.37(7)	74.18
O2-Sb1-O3×2	80.26(8)	81.20
O2-Sb1-O4×2	141.81(9)	143.68
O2-Sb1-O4×2	84.29(12)	82.19
O3-Sb1-O3	143.04(15)	144.78
O3-Sb1-O4×2	68.99(4)	70.28
O3-Sb1-O4×2	139.07(2)	136.35
O4-Sb1-O4	71.93(17)	67.64
Sb1-O2-Sb1	145.5(2)	147.5
Sb1-O2-H6	111.9(2)	108.16
Sb1-O2-H6	99.6(2)	104.08
Sb1-O3-C5	119.5(2)	115.72
Sb1-O4-C5	121.4(2)	118.81
O3-C5-O4	130.2(3)	125.05
O3-C5-C5	113.9(5)	118.19
O4-C5-C5	115.8(5)	116.75

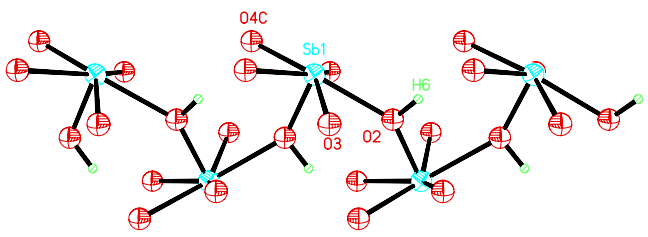

Figure 3. (Color online) The zigzag hydroxyl-bridged chains along the a axis in $Sb(C_2O_4)OH$. 50% probability ellipsoids/spheroids.

https://doi.org/10.1154/1.3308616 Published online by Cambridge University Press

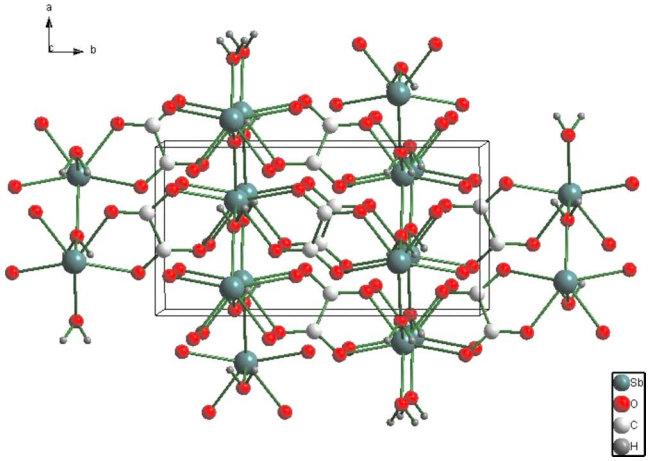

Figure 4. (Color online) The crystal structure of $Sb(C_2O_4)OH$, viewed approximately along the *c* axis.

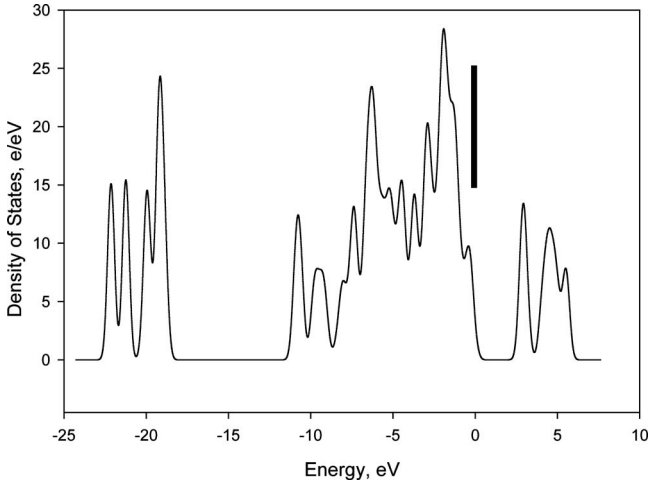

Figure 6. The density of states plot for $Sb(C_2O_4)OH$. The heavy vertical line segment indicates the Fermi level.

(Figure 5) makes it appear that there are voids, no voids are detected by Mercury (Macrae *et al.*, 2008) and none are apparent in a space-filling rendering.

The density of states plot (Figure 6) makes it clear that the compound is an insulator. The highest occupied molecular orbital (HOMO) consists of the Sb lone pairs, which "fill" the apparent "void" (Figure 7). The next lowest-energy filled orbitals are oxygen *p* orbitals.

The bischelating oxalate bridging of two Sb observed in this compound is the most common binding mode in antimony oxalates (Udovenko *et al.*, 1981b; Southerington *et al.*, 1991; Schwarz *et al.*, 1981; Coudreau-Ducourant *et al.*, 1981; Millington and Sowerby, 1992). Also observed are single chelation (Poore and Russell, 1971; Millington and Sowerby, 1992), chelation to one Sb and monodentate binding to another (Udovenko *et al.*, 1981a; Davidovich *et al.*, 1983), and *trans*-monodentate bridging of two Sb (Davidovich *et al.*, 1983; Escande *et al.*, 1978a, 1978b; Marsh, 1997).

$Sb(C_2O_4)OH$ is isostructural to $Bi(C_2O_4)OH$, the structure of which was determined recently using single crystal techniques (Rivenet *et al.*, 2008). The analogy was not detected by a default reduced cell search in the Inorganic Crystal Structure Database (Hellenbrandt, 2004); the tolerances on the unit cell edges had to be increased from 0.1 to 0.3 Å. The Bi coordination sphere is described as having six normal bonds and two long "secondary" bonds. Both bond valence considerations and Mulliken overlap populations suggest that the long (3.18 Å) Sb-O distances in this compound do not represent real bonds.

The Bravais-Friedel-Donnay-Harker morphology (Donnay and Harker, 1937) calculated from the crystal structures is blocky, but possibly consistent with elongated morphology along [100], or platy with {010} or {001} as prominent faces. Analysis of the calculated pole figure plots suggests a platy morphology with {001} as the large faces. The refined texture index is 1.441. Although not obvious from the pattern, preferred orientation is significant and made the structure solution very difficult. Undetected preferred orientation can be

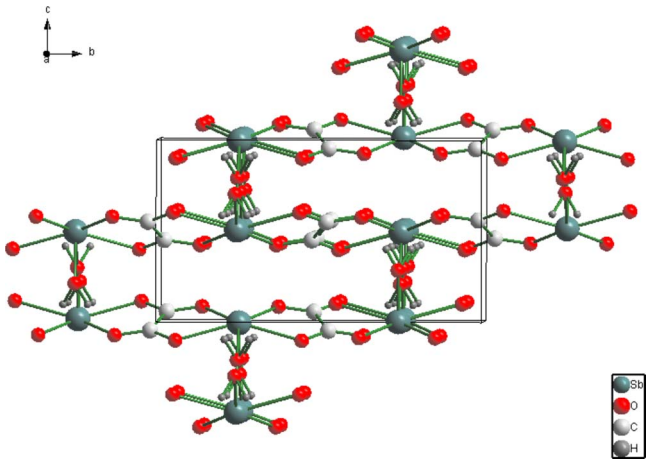

Figure 5. (Color online) The crystal structure of $Sb(C_2O_4)OH$, viewed approximately along the *a* axis.

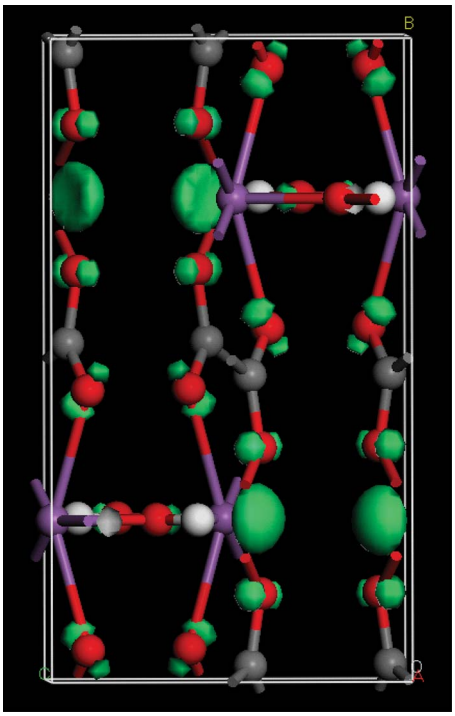

Figure 7. (Color online) The HOMO, illustrating the Sb^{3+} lone pairs.

https://doi.org/10.1154/1.3308616 Published online by Cambridge University Press

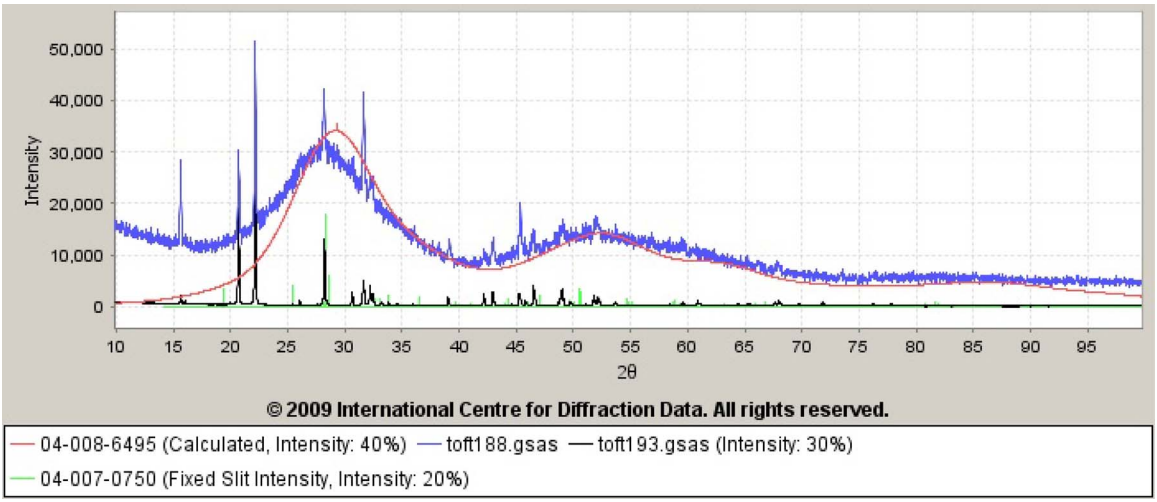

Figure 8. (Color online) The powder pattern (blue) of $Sb(C_2O_4)OH$ after refluxing in water, illustrating the conversion to nanocrystalline cervantite (Sb_2O_4, PDF entry 04-008-6495, red) and a trace of valentinite (Sb_2O_3, green). Only a small concentration of antimony oxalate hydroxide (black) remained.

fatal to *ab initio* structure solution, resulting in collapsing of electron density into a plane.

Refluxing $Sb(C_2O_4)OH$ in water converts it into nanocrystalline cervantite (Sb_2O_4) with a trace of Sb_2O_3 (Figure 8). The decomposition under relatively mild conditions shows that $Sb(C_2O_4)OH$ can be a useful reagent.

IV. SUMMARY

The crystal structure of $Sb(C_2O_4)OH$ has been solved by applying charge flipping and difference Fourier techniques to laboratory X-ray powder data exhibiting significant preferred orientation and refined by the Rietveld method. The structure is chemically reasonable compared to other antimony oxalates and to $Bi(C_2O_4)OH$. The experimental powder pattern has been submitted to ICDD for inclusion in future releases of the Powder Diffraction File.

Ambe, S. (**1975**). "Chemical properties of antimony(III) oxalate hydroxide," J. Inorg. Nucl. Chem. **37**, 2023.

Brese, N. E. and O'Keefe, M. (**1991**). "Bond-valence parameters for solids," Acta Crystallogr., Sect. B: Struct. Sci. **B47**, 192–197.

Brown, I. D. (**2002**). *The Chemical Bond in Inorganic Chemistry: The Bond Valence Model* (Oxford University Press, Oxford).

Bruno, I. J., Cole, J. C., Kessler, M., Luo, Jie, Motherwell, W. D. S., Purkis, L. H., Smith, B. R., Taylor, R., Cooper, R. I., Harris, S. E., and Orpen, A. G. (**2004**). "Retrieval of crystallographically-derived molecular geometry information," J. Chem. Inf. Comput. Sci. **44**, 2133–2144.

Clark, S. J., Segall, M. D., Pickard, C. J., Hasnip, P. J., Probert, M. J., Refson, K., and Payne, M. C. (**2005**). "First principles methods using CASTEP," Z. Kristallogr. **220**, 567–570.

Coudreau-Ducourant, D., Ducourant, B., Fourcade, R., and Mascherpa, G. (**1981**). "New complex of antimony oxide fluoride and oxalate: Crystal structure of $(NH_4)_4H_2(C_2O_4)_3(SbOF)_2 \cdot 2H_2O$," Z. Anorg. Allg. Chem. **476**, 229–236 (CSD Refcode OXFLSB).

Davidovich, R. L., Zemnukhova, L. A., Udovenko, A. A., and Sigula, N. I. (**1983**). "Synthesis and structure of rubidium oxalatofluorodiantimonates(III)," Koord. Khim. **9**, 787–792 (CSD Refcodes CANRIS, CANROY, and CANRUE).

Donnay, J. D. H. and Harker, D. (**1937**). "A new law of crystal morphology extending the law of Bravais," Am. Mineral. **22**, 446–467.

Escande, P., Tichit, D., Ducourant, B., Fourcade, R., and Mascherpa, G. (**1978a**). "Interaction between the lone electronic pair and π bond in a nonsymmetric system: Crystal structure of sodium oxalate-antimony trifluoride ($Na_2C_2O_4(SbF_3)_2$)," Ann. Chim. (Paris) **3**, 117–124 (CSD Refcode SBFOXS).

Escande, P., Tichit, D., Ducourant, M. B., Fourcade, R., and Mascherpa, G. (**1978b**). "Interaction paire electronique libre-liaison pi dans un systeme non symetrique: Structure cristalline de $Na_2C_2O_4(SbF_3)_2$," Ann. Chim. (Paris) **3**, 124–124 (ICSD collection code 200225).

Faber, J. and Fawcett, T. (**2002**). "The Powder Diffraction File: Present and future," Acta Crystallogr., Sect. B: Struct. Sci. **58**, 325–332.

Hellenbrandt, M. (**2004**). "The Inorganic Crystal Structure Database (ICSD)—Present and future," Crystallogr. Rev. **10**, 17–22.

Karlov, V. P., Butuzov, G. N., and Dobrokhotova, T. F. (**1983**). "Preparation and some properties of antimony(III) oxalate," Zh. Neorg. Khim. **28**, 2145–2146 (PDF entry 00-037-0646).

Korzun, B. B., Schorr, S., Schmitz, W., Fadzeyeva, A. A., Kommichau, G., and Bente, K. (**2005**). "Preparation of $BaBi_{1/2}Sb_{1/2}O_3$ from $Ba(COO)_2 \cdot 0.5H_2O$ and $Sb(COO)_2(OH)$ oxalates and Bi_2O_3 oxide," J. Cryst. Growth **277**, 205–209.

Larson, A. C. and Von Dreele, R. B. (**2004**). General Structure Analysis System (GSAS), Report LAUR 86-748, Los Alamos National Laboratory, Los Alamos, NM.

Le Bail, A. (**2008**). "The profile of a Bragg reflection for extracting intensities," in *Powder Diffraction: Theory and Practice*, edited by R. E. Dinnebier and S. J. L. Billinge (Royal Society of Chemistry, Cambridge), pp. 134–165.

Louër, D. and Boultif, A. (**2007**). "Powder pattern indexing and the dichotomy algorithm," Z. Kristallogr. **26**, 191–196.

Macrae, C. F., Bruno, I. J., Chisholm, J. A., Edgington, P. R., McCabe, P., Pidcock, E., Rodriguez-Monge, L., Taylor, R., van de Streek, J., and Wood, P. A. (**2008**). "Mercury CSD 2.0—New features for the visualization and investigation of crystal structures," J. Appl. Crystallogr. **41**, 466–470.

Marsh, R. E. (**1997**). "The perils of *Cc* revisited," Acta Crystallogr., Sect. B: Struct. Sci. **53**, 317–322 (CSD Refcode SBFOXS01).

Materials Data, Inc. (**2008**). JADE 8.5, computer software, Livermore, CA.

Millington, P. L. and Sowerby, D. B. (**1992**). "Phenylantimony(V) oxalates: Isolation and crystal structures of $[SbPh_4][SbPh_2(ox)_2]$, $[SbPh_3(OMe)]_2ox$ and $[SbPh_4]_2ox$," J. Chem. Soc. Dalton Trans. 1199–1204 (CSD Refcodes PABTAN, PABTER, and PABTIV).

Oszlányi, G. and Sütó, A. (**2008**). "The charge flipping algorithm," Acta Crystallogr., Sect. A: Found. Crystallogr. **64**, 123–134.

Petříček, V., Dušek, M., and Palatinus, L. (**2006**). JANA2006, the crystallographic computing system, computer software, Institute of Physics, Praha, Czech Republic.

Poore, M. C. and Russell, D. R. (**1971**). "Crystal structure of the trisoxalatoantimonate(III) ion: Sterically-active lone pair in six-coordination," J. Chem. Soc. D 18–19 (CSD Refcodes AMSBOX and KSBOXL).

Rietveld, H. M. (**1969**). "Line profile refinement method for nuclear and magnetic structures," J. Appl. Crystallogr. **2**, 65–71.

Rivenet, M., Roussel, P., and Abraham, F. (**2008**). "One-dimensional inorganic arrangement in the bismuth oxalate hydroxide $Bi(C_2O_4)OH$," J.

Solid State Chem. **181**, 2586–2590 (ICSD collection code 419313).
Schwarz, W., Schmidt, A., and Blösl, S. (**1981**). "Reaction of the 1:1 addition compound of antimony(V) chloride and water with oxalic or squaric acid," Z. Anorg. Allg. Chem. **477**, 113–118 (CSD Refocde OCOXSB).
Sidey, V. (**2009**). "The alternative presentation of the Brown-Wu bond-valence parameters for some s2-cation/O^{2-} ion pairs," Acta Crystallogr., Sect. B: Struct. Sci. **65**, 99–101.
Southerington, I. G., Begley, M. J., and Sowerby, D. B. (**1991**). "A new diphenylantimony oxide containing a planar Sb_6O_6 ring," J. Chem. Soc., Chem. Commun. 1555–1556 (CSD Refocde JODLET).
Stephens, P. W. (**1999**). "Phenomenological model of anisotropic broadening in powder diffraction," J. Appl. Crystallogr. **32**, 281–289.
Udovenko, A. A., Sigula, N. I., and Davidovich, R. L. (**1981a**). "Crystal structure of cesium dioxalatotetrefluorodiantimonate(III) monohydrate," Koord. Khim. **7**, 1708–1712 (CSD Refcode BAYLUI).
Udovenko, A. A., Sigula, N. I., Samarets, L. V., and Davidovich, R. L. (**1981b**). "Crystal structure of ammonium trioxalatotetrefluorodiantimonate(III) dihydrate," Koord. Khim. **7**, 450–454 (CSD Refcode FLOXSB).

https://doi.org/10.1154/1.3308616 Published online by Cambridge University Press